

A Monte Carlo test of the Fisher–Nakanishi–Scaling theory for the capillary condensation critical point

Oliver Dillmann

Institut für Physik, Johannes-Gutenberg-Universität Mainz, D-55099 Mainz, Staudinger Weg 7, Germany

Wolfgang Janke^{a)}

Institut für Theoretische Physik, Universität Leipzig, D-04109 Leipzig, Augustusplatz 10/11, Germany

Marcus Müller and Kurt Binder^{b)}

Institut für Physik, Johannes-Gutenberg-Universität Mainz, D-55099 Mainz, Staudinger Weg 7, Germany

(Received 13 October 2000; accepted 2 January 2001)

Extending the Swendsen–Wang cluster algorithm to include both bulk (H) and surface fields (H_1) in $L \times L \times D$ Ising films of thickness D and two free $L \times L$ surfaces, a Monte Carlo study of the capillary condensation critical point of the model is presented. Applying a finite-size scaling analysis where the lateral linear dimension L is varied over a wide range, the critical temperature $T_c(D)$ and the associated critical field $H_c(D)$ are estimated for $4 \leq D \leq 32$ lattice spacings, for a choice of the surface field H_1 small enough that the dependence of $H_c(D)$ on H_1 is still linear. It is shown that the results are consistent with the power laws predicted by Fisher and Nakanishi [M. E. Fisher and H. Nakanishi, *J. Chem. Phys.* **75**, 5857 (1981)], namely $T_c(\infty) - T_c(D) \propto D^{-1/\nu}$, $H_c(D) \propto D^{-(\Delta - \Delta_1)/\nu}$, where ν is the bulk correlation length exponent of the three-dimensional Ising model, and Δ , Δ_1 are the corresponding ‘‘gap exponents’’ associated with bulk and surface fields, respectively. As expected, the order parameter of the thin film near its critical point exhibits critical behavior compatible with the universality class of the two-dimensional Ising model. © 2001 American Institute of Physics. [DOI: 10.1063/1.1350574]

I. INTRODUCTION

The application prospects of nanoscale technology have created a fresh interest in the behavior of both simple fluids and complex fluids confined in pores or in a thin film geometry in layers confined by parallel walls.^{1–5} However, a prerequisite for the clarification of pattern formation^{2,3} and dynamics^{4,5} is a good understanding of the interplay between bulk and surface effects on thermodynamics and phase behavior in this finite-size geometry:^{6–8} although theoretical aspects of phase transitions and critical phenomena in confined geometry have been considered for a long time,^{9–28} this is still a topic of active current research^{29–33} even for one of the most well-known phenomena, namely ‘‘capillary condensation.’’^{34,35} By capillary condensation one means the finding, already discovered in the 19th century,³⁴ that in a capillary the condensation of a gas occurs already at a lower pressure p than the coexistence pressure p_{coex} necessary to induce condensation in the bulk. Qualitatively, this shift of the transition can be attributed to the interaction of the fluid molecules with the attractive walls of the capillary. Although confinement effects on fluids and their phase transitions have been studied experimentally for a long time as well,^{36–49} a quantitative characterization of the shift of the capillary condensation critical point remains a challenge. While for temperatures T below the critical temperature $T_c(D)$ of the thin film of thickness D the chemical potential at the condensation transition $\mu_c(D)$ is shifted relative to its bulk value

simply as $\mu_c(D) - \mu_c(\infty) \propto D^{-1}$ (‘‘Kelvin equation’’),²⁷ for large enough D , Fisher and Nakanishi¹⁶ predicted a completely different power law for the corresponding shift at the critical temperature itself, namely

$$\mu_c(D) - \mu_c(\infty) \propto D^{-(\Delta - \Delta_1)/\nu}, \quad T = T_c(D) \quad (1)$$

for weak surface forces. In Eq. (1), critical exponents of the three-dimensional Ising model universality class (that encompasses criticality of gas–fluid critical points or the related unmixing transitions in binary mixtures, etc.) enter, namely the correlation length exponent⁵⁰ $\nu \approx 0.63$ and the ‘‘gap exponent’’ $\Delta = \gamma + \beta \approx 1.56$ and the corresponding exponent for a free surface^{19,51–53} $\Delta_1 \approx 0.46–0.48$. Also for the shift of T_c a similar power law holds

$$T_c(\infty) - T_c(D) \propto D^{-1/\nu}, \quad (2)$$

which is the same relation as is familiar from standard finite-size scaling^{10,18,54,55} for the shift of T_c in films with ‘‘neutral walls’’ [i.e., no surface field preferring one of the phases coexisting for $T < T_c(D)$ at $\mu_c(D) \equiv \mu_c(\infty)$ act] or in films with periodic boundary conditions where surface effects are *a priori* absent. While for the latter systems Eq. (2) has been studied by various methods,^{13,15,56–60} Eq. (1) has not yet been tested by Monte Carlo simulations. In previous work,^{26,28,29} tests of the Kelvin equation and corrections to it⁶¹ have been carried out and a capillary condensation critical point was located for a thin Ising film²⁸ but for a single value of D only.

In the present paper, we fill in this gap by presenting a Monte Carlo study of the critical behavior of capillary condensation in thin Ising films for a range of thicknesses. In-

^{a)}Electronic mail: Wolfgang.Janke@itp.uni-leipzig.de

^{b)}Electronic mail: Kurt.Binder@uni-mainz.de

voking the universality principle,⁶² one can argue that nearest neighbor Ising lattices with short range surface fields should yield the same power law, Eq. (1), as more realistic models and real fluids in slit-like capillaries do. Unlike the situation in real fluids, packing effects at the surfaces and a dependence of the density in the middle of the film on its thickness are, however, absent and one focuses on the universal critical behavior. One can argue that the order parameter correlations in the directions parallel to the wall should all scale with the critical exponents of the universality class of the two-dimensional Ising model⁶²

$$M \propto \tilde{t}^{\beta_2}, \quad \chi \propto |\tilde{t}|^{-\gamma_2}, \quad \xi_{\parallel} \propto |\tilde{t}|^{-\nu_2}, \quad \beta_2 = 1/8, \\ \gamma_2 = 7/4, \quad \nu_2 = 1, \\ \tilde{t} \equiv 1 - T/T_c(D) \rightarrow 0, \quad \text{all } D < \infty. \quad (3)$$

Of course, one expects that for large D the asymptotic critical region where this two-dimensional critical behavior holds is very narrow, due to a crossover to the three-dimensional critical behavior as $D \rightarrow \infty$, and a quantitative understanding of this crossover^{13,56-58} is a challenging aspect of this problem, too.

In Sec. II, we shall, hence, briefly define the model that is studied and the quantities that will be analyzed and comment on the simulation methods. Section III briefly reviews the scaling predictions, including the finite-size scaling results for the case where both D and the lateral linear dimension L are finite. Section IV then presents our results on $T_c(D)$ and the critical fields $H_c(D)$, on which our tests of Eqs. (1) and (2) are based. Section V discusses those aspects of our results which are pertinent to a test of two-dimensional criticality, Eq. (3), while Sec. VI summarizes our conclusions.

II. MODEL AND SIMULATION TECHNIQUE

Invoking the well-known isomorphism between the lattice gas model of fluids and the Ising model of magnetism (see, e.g., Ref. 28 for details), we study the Ising model on the simple cubic lattice in the presence of a bulk field H and a surface field H_1 :

$$\mathcal{H} = -J \sum_{\langle i,j \rangle} S_i S_j - H \sum_i S_i - H_1 \sum_{i \in \text{surfaces}} S_i, \quad S_i = \pm 1, \quad (4)$$

where the exchange interaction J is only present between nearest neighbors on the lattice. Note that phase coexistence in the bulk [phases with positive and negative magnetization correspond to gas and liquid phases of the fluid, respectively] corresponds to $H=0$, see Fig. 1. In the thin film, one trivially obtains the result that for zero temperature phase coexistence occurs for²⁸ $H_{\text{coex}}(D, T=0) = -2H_1/D$, but for $T > 0$ the variation of $H_{\text{coex}}(D, T)$ is nontrivial. While previous work²⁸ was mostly interested in the behavior of $H_{\text{coex}}(D, T)$ near the temperature $T_w(H_1)$ of the wetting transition,^{1,6,7,63} we consider here scaled surface fields $H_1 D^{\Delta_1/\nu}$ small enough such that we stay in the nonwet regime of the surface phase diagram of the semi-infinite system⁶⁴ throughout, although we consider the vicinity of $T_c^\infty = T_c(D=\infty)$. Measuring all

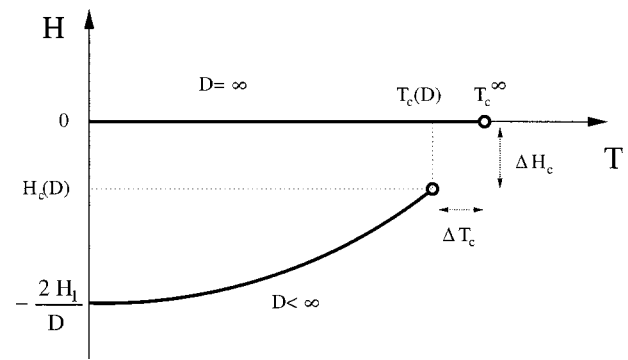


FIG. 1. Schematic phase boundary for an Ising film of thickness D , where on both surfaces a field H_1 acts, in the plane of variables temperature T and bulk field H .

lengths in units of the lattice spacing, we consider film thicknesses $D=4, 8, 12, 16, 24, 28$, and 32 for an $L \times L \times D$ geometry, varying L over an as wide range as is practical, from the point of view of available computer resources. In the x, y directions parallel to the thin film, we apply periodic boundary conditions as usual.^{13,28}

In order to be able to find $T_c(D)$ and $H_c(D) \equiv H_{\text{coex}}(D, T=T_c(D))$ reliably, we have to use aspect ratios $L/D \gg 1$. Although the choices of film thickness as quoted above are not extremely large, it is clear that use of rather large linear dimensions L is mandatory for obtaining reliable results. If we would use the Metropolis algorithm,⁶⁵⁻⁶⁷ as done in Refs. 13 and 28, or the heatbath algorithm,⁶⁷ ‘‘critical slowing down’’^{66,67} would be a serious problem: i.e., the ‘‘time’’ τ over which subsequently generated system configurations are correlated varies as⁶⁷

$$\tau \propto L^z \quad \text{with } z \approx 2.16 (d=2) \text{ or } z \approx 2.03 (d=3), \quad (5)$$

the prefactor in this power law being of order unity if Monte Carlo time is measured in units of attempted Monte Carlo steps (MCS) per spin. Since we wish to use linear dimensions of the order of $L \approx 10^2$, relaxation times of the order of 10^4 MCS easily result. Given the fact that quantities like the specific heat C_v and the susceptibility χ , recorded from fluctuations of energy and magnetization

$$C_v = (\langle \mathcal{H}^2 \rangle - \langle \mathcal{H} \rangle^2) / (L^2 D k_B T^2), \\ \chi = \left[\left\langle \left(\sum_i S_i \right)^2 \right\rangle - \left\langle \sum_i S_i \right\rangle^2 \right] / (L^2 D k_B T), \quad (6)$$

are nonself-averaging,⁶⁶⁻⁶⁸ one needs $n \gg 1$ statistically independent observations (i.e., separated by time intervals $\Delta t > \tau$) to obtain C_v and χ with small enough error (the relative error of these quantities is⁶⁸ $\sqrt{2/n}$, irrespective of L and D). For this reason, it is clear that the use of cluster algorithms which reduce critical slowing down^{67,69-75} is highly desirable. However, for the present problem where both a bulk magnetic field and a surface magnetic field of competing sign are present [Eq. (4)] application of cluster algorithms is nontrivial. It turns out that an extension of the ‘‘ghost spin algorithm’’⁷¹⁻⁷³ to the present problem is rather straightforwardly possible.^{76,77} The coupling of spins to a magnetic field is thereby treated as if it were an additional infinite-

range exchange coupling to an extra spin $S_G = \pm 1$. This coupling has the strength $h = |H|$ for spins in the interior of the film and $h = |H_1 + H|$ for spins in the surface layers. In addition to putting bonds in clusters of spins (inside a cluster all spins are connected by exchange interactions and have the same sign) with probability^{69–77} $p_B = 1 - \exp(-2J/k_B T)$ one also puts bonds between the spins in clusters and the ghost spin $p_G = 1 - \exp(-2h/k_B T)$, if the orientation of the spins in the cluster is the same as that of the ghost spin [which is $S_G = \text{sign}(H)$ for interior spins and $S_G = \text{sign}(H_1 + H)$ for spins in the surface planes, respectively].

While this extension of the cluster algorithm to the case of nonzero bulk and surface fields is formally exact, discussion of its efficiency is a rather delicate problem: in fact, if $h/k_B T$ is of order unity, also p_G is of order unity and the infinite-range character of this coupling then implies that huge clusters containing a large fraction of the entire simulation volume would be created most of the time! It is clear that under such circumstances the algorithm would be very inefficient; as in the case of zero field it is necessary for a good performance of a cluster algorithm that typically large clusters are created but a single large cluster must contain only a negligible fraction of the total volume in the thermodynamic limit. As a consequence, one needs $h/k_B T \ll 1$, and since $k_B T$ is in the range of 3.5–4.5 we have thus chosen to work with a single value of the surface field, namely $H_1 = -0.015J$. Even for this small value—note that the corresponding value of H is typically one or two orders of magnitude smaller, see later—the performance of the algorithm has significantly deteriorated, in comparison with the case without any magnetic fields. This fact can be clearly demonstrated by a binning analysis^{75,78} of the magnetization m in the system: the N (dynamically correlated) subsequent observations $m_\nu = (1/N) \sum_{i=1}^N S_i^\nu$ are grouped into $n = N/N_b$ blocks of length N_b , from which block averages \tilde{m}_μ of the corresponding N_b observations $\{m_\nu\}$ belonging to the block with index μ are formed. Then

$$\Delta m \equiv [n(n-1)]^{-1/2} \sqrt{\sum_{i=1}^n (\tilde{m}_\mu - \tilde{m})^2}, \quad (7)$$

(where $\tilde{m} = n^{-1} \sum_{i=1}^n \tilde{m}_i$) is studied as a function of block length N_b (Fig. 2): when Δm is independent of N_b , the subsequent \tilde{m}_μ are statistically independent, and Δm is a good estimation of the statistical error; otherwise one sees a systematic increase of Δm with N_b and the value of N_b needed to reach a saturation value yields an estimate for the correlation time. For the Metropolis algorithm and the chosen system size ($L=128$), even for $N_b=4000$ one is far from saturation, and hence, it is clear that this algorithm would be very impractical for the present problem. For the cluster algorithm and $H_1=0$, on the other hand, Δm vs N_b is essentially constant, $\Delta m \approx 0.0004$, the correlation time being of order unity, as expected.^{67,69,74,75} However, this is not so for the cluster algorithm in the case $H_1 = -0.015$: Δm saturates at a plateau of about $\Delta m \approx 0.007$, i.e., the error is almost a factor 20 larger, and the correlation time is of the order of $\tau_m \approx 280$ Monte Carlo steps in the example shown in Fig. 2(b). Thus, while the gain of the cluster algorithm in the

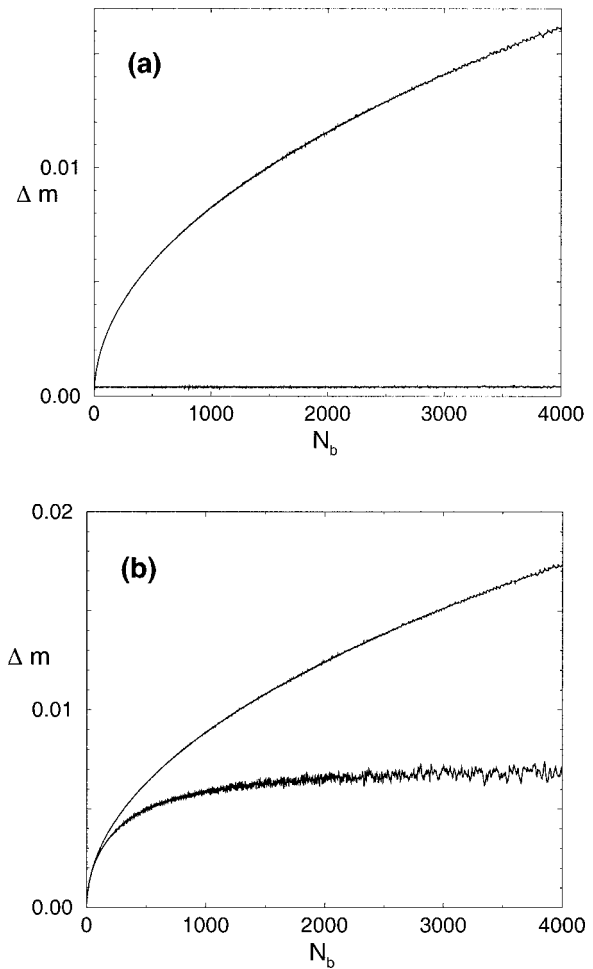


FIG. 2. Error Δm as calculated from Eq. (7) plotted vs block length N_b for the case $D=32$, $L=128$, and two choices of H_1 , $H_1=0$ (a) and $H_1 = -0.015J$ (b). In both cases the chosen temperature [and bulk field H in the case of (b)] are adjusted such that the system is precisely at the critical point. Upper curve in each panel represents the Metropolis algorithm, lower curve represents the cluster algorithm.

zero field case compared to the Metropolis algorithm is very significant, in our problem it is only rather modest! This—somewhat unexpected—dramatic decrease of the efficiency of the cluster algorithm with increasing strength of the surface (and bulk) fields has prevented us both from studying systems larger than $L=128$ and from studying the dependence on H_1 systematically. Runs of length up to 1.2 million Monte Carlo steps were performed.

As is well known,^{67,75,79} cluster algorithms at critical points of Ising systems are rather sensitive to correlations among the pseudorandom numbers produced by the random number generator. In the present work, we used thus an improved version of the standard ‘‘R250’’ generator,⁸⁰ where two versions [one based on the pair of integers (250, 103) the other with the pair (521, 168)] are combined with the logical exclusive OR (XOR) operation.

In order to make best use of our simulation data, we apply standard multihistogram interpolation techniques.^{67,74,75,81} Note that we needed a three-dimensional histogram $P(E, m, m_1)$, E being the exchange energy, m_1 the magnetization in the surface plane, in order to allow re-

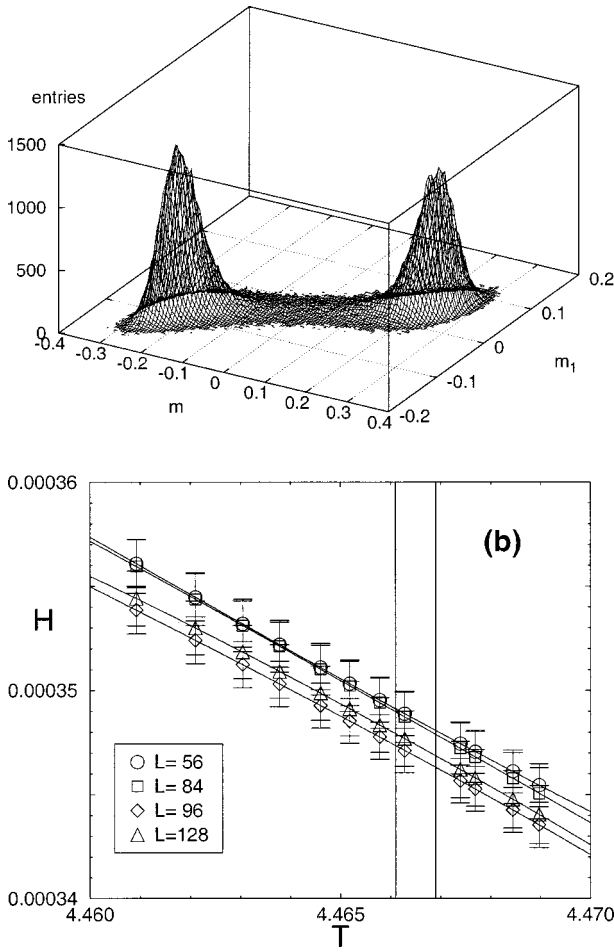


FIG. 3. (a) Unnormalized histogram $P(m, m_1)$ of the system with $D=32$, $L=96$, $H_1/J=-0.015$, $H/J=0.00028$ at $k_B T/J=4.471$, which is a state close to the two-phase coexistence line. (b) Two-phase coexistence line in the plane of variables H/J and $k_B T/J$ for $D=28$, estimated separately for four different choices of L from the “equal weight” rule, showing also the statistical errors as estimated from Jackknife procedures (see Ref. 83). The two vertical lines show the error interval of the critical temperature.

weightings in the full parameter space of independent control variables (T, H, H_1) and, hence, the storage requirements for P are nontrivial. However, noting that all measurements of E, m, m_1 can be represented by integers, each integer needing 4 byte, we can store the time series of 10^6 observations with a storage of 12 Mbyte, irrespective of the choices of L and D .

The multihistogram reweighting with respect to the bulk field H is crucial in order to be able to find the field $H_{\text{coex}}(T)$, along which for $T < T_c(D)$ two-phase coexistence occurs, applying the “equal weight rule.”^{66,67,75,82} In the space of variables (E, m, m_1) , the two phases show up as separate peaks of $P(E, m, m_1)$ [or $P(m, m_1)$, respectively, see Fig. 3(a), when one studies an isotherm one can integrate out E , of course], which have precisely the same weight at $H = H_{\text{coex}}(T)$ while for $H \neq H_{\text{coex}}(T)$ (but not too far away from it) the two peaks can still be identified but have different weight. With the multihistogram reweighting, a small number of simulation points suffices to generate the curve $H_{\text{coex}}(T)$ [and its extrapolation into the regime $T > T_c(D)$] with reasonable precision, see Fig. 3(b). Since near $T_c(D)$ the free energy differences between the two phases are very

small also off coexistence, the statistical error in the estimation of $H_{\text{coex}}(T)$ is not negligible, and also systematic errors, since L/D is not large enough, need to be considered. The latter problem also affects the estimation of $T_c(D)$, as will be discussed in Sec. IV.

III. SCALING PREDICTIONS

For completeness, we first summarize the pertinent predictions of the scaling theory for thin Ising films near the critical point,^{16–19,84} assuming the lateral linear dimension L infinite, and consider the extension⁵⁸ to finite L in the following. The singular part of the free energy per spin is assumed to scale as follows:

$$f_{\text{sing}}(D, T, H, H_1) \approx |t|^{2-\alpha} \tilde{f}_{\pm}(D|t|^{\nu}, H|t|^{-\Delta}, H_1|t|^{-\Delta_1}), \quad (8)$$

where α is the exponent of the specific heat of the three-dimensional Ising model, $t = [T - T_c(\infty)]/T_c(\infty)$, \tilde{f}_{\pm} is a “scaling function” (with two different branches, referring to the sign of t), and the other exponents have already been defined in Sec. I.

Now it is convenient to introduce the scaling variables

$$x \equiv D|t|^{\nu}, \quad w \equiv H_1 D^{\Delta_1/\nu}, \quad (9)$$

and then Eq. (8) can also be written as, eliminating $|t|$ from the arguments of \tilde{f}_{\pm} ,

$$f_{\text{sing}}(D, T, H, H_1) \approx |t|^{2-\alpha} \tilde{f}_{\pm}\left(x, \frac{HD^{\Delta/\nu}}{x^{\Delta/\nu}}, \frac{w}{x^{\Delta_1/\nu}}\right). \quad (10)$$

Since the critical point of the thin film is shifted relative to the bulk critical point $T_c(\infty)$, it must correspond to a singular behavior of the scaling function \tilde{f}_{\pm} . At fixed H_1 and fixed D this means the scaling function $\tilde{f}_{\pm}(x, y, y_1 = w/x^{\Delta_1/\nu})$ has a singularity at a point $x_c(w), y_c(w)$. Therefore, the shifts $\Delta T_c(D), \Delta H_c(D)$ follow as¹⁶

$$\Delta T_c = T_c(D, H_1) - T_c(\infty) = -B_T D^{-1/\nu} X_c(CH_1 D^{\Delta_1/\nu}), \quad (11)$$

$$\Delta H_c \equiv H_c(D, H_1) = -B_H D^{-\Delta/\nu} Y_c(CH_1 D^{\Delta_1/\nu}). \quad (12)$$

The scaling functions X_c and Y_c are universal, while B_T , B_H , and C are nonuniversal critical amplitudes, which are normalized such that $X_c(Cw) = 1 + (Cw)^2 + \dots$, $Y_c(Cw) \approx Cw + 0(Cw)^3$. Note that both functions are analytic for $w \rightarrow 0$, and ΔT_c should be an even function of H_1 and, hence, w , while ΔH_c must be an odd function of H_1 . From these considerations, for small H_1 Eqs. (1) and (2) result, remembering²⁸ that $\mu_c(D) - \mu_c(\infty) = -2H_c$.

An alternative argument for Eq. (1), which also elucidates how this equation fits together with the Kelvin equation ($H_c - H_1/D$) in the critical region for large enough D , derives from a consideration of phase coexistence for temperatures slightly below $T_c(D)$. If $H_1 = H = 0$, we would have two coexisting phases with magnetization profiles $m^+(z)$ and $m^-(z) = -m^+(z)$ across the film, and both states have the same free energy $F_+(0,0) = F_-(0,0)$. Since these profiles are smooth functions of H and H_1 , an expansion of the free energies around $F_+(0,0)$ [or $F_-(0,0)$, respectively] yields

$$\begin{aligned}
 -\Delta F_+ &\equiv F_+(0,0) - F_+(H, H_1) \\
 &= \overline{m^+} HDL^2 + 2m_1^+ H_1 L^2, \tag{13}
 \end{aligned}$$

$$\begin{aligned}
 -\Delta F_- &\equiv F_-(0,0) - F_-(H, H_1) \\
 &= \overline{m^-} HDL^2 + 2m_1^- H_1 L^2, \tag{14}
 \end{aligned}$$

where $\overline{m^+}$ and $\overline{m^-}$ refer to the average over the magnetization profile in the respective states, and m_1^+ and m_1^- the layer magnetizations in the surface layer. To leading order for small H_1 and small H in Eqs. (13) and (14), $\overline{m^+}$, $\overline{m^-}$ and m_1^+ , m_1^- are to be taken at zero fields, and thus satisfy the symmetry $\overline{m^-} = -\overline{m^+}$ and $m_1^- = -m_1^+$. Phase coexistence occurs for $\Delta F^+ = \Delta F^-$, and hence the Kelvin equation results

$$H_{\text{coex}}(D, T, H_1) \approx -\frac{2H_1}{D} \frac{m_1^+(D, T)}{m^+(D, T)}. \tag{15}$$

Assuming then that $D \gg \xi$, the correlation length in the bulk, $m^+(z)$ will approach the bulk spontaneous magnetization $m_b = \hat{B}_b(-t)^\beta$ almost everywhere, and hence, $\overline{m^+} \approx \hat{B}_b(-t)^\beta$, \hat{B}_b being the respective critical amplitude. Likewise $m_1^+(D, T)$ approaches the surface layer magnetization of a semi-infinite system^{19,51,84} $m_1 = \hat{B}_1(-t)^{\beta_1}$, with \hat{B}_1 the corresponding amplitude. Therefore, Eq. (15) becomes in this limit

$$H_{\text{coex}}(D, T, H_1) \approx -\frac{2H_1}{D} \frac{\hat{B}_1}{\hat{B}_b} (-t)^{\beta_1 - \beta}, \quad x = D|t|^\nu \rightarrow \infty. \tag{16}$$

Since⁵⁰ $\beta \approx 0.325$ and^{19,51-53} $\beta_1 \approx 0.78-0.80$, we see that the coefficient of the term H_1/D in Eq. (16) gets smaller and smaller as $|t|$ gets smaller. Due to this vanishing coefficient in the limit $|t| \rightarrow 0$ a smooth crossover between the Kelvin equation, Eqs. (15) and (16), and Eq. (1) becomes possible. Remembering that for D finite there is a shift of T_c as given by Eq. (2), we can further conclude that the critical field should be of the order

$$\begin{aligned}
 H_c(D_1, H_1) &\equiv H_{\text{coex}}(D, T_c(D), H_1) \\
 &\propto -\frac{2H_1}{D} D^{-(\beta_1 - \beta)/\nu} = -2H_1 D^{-(\Delta - \Delta_1)/\nu}, \tag{17}
 \end{aligned}$$

where in the last step the standard scaling relations $\beta = 2 - \alpha - \Delta$, $\beta_1 = 2 - \alpha - \nu - \Delta_1$ were used. Eq. (17) obviously is nicely compatible with Eq. (1).

Equation (16) allows an interesting conclusion to be drawn on the slope of the coexistence curve at the critical point of the film (cf. Fig. 1). We find first for the angle $\theta(t)$ describing this slope for $T < T_c(D)$:

$$\begin{aligned}
 \tan(\theta) &\equiv (\partial H / \partial T)_{H_1} \\
 &= \frac{2H_1}{T_c(\infty)} \frac{\beta_1 - \beta}{D} \frac{\hat{B}_1}{\hat{B}_b} (-t)^{\beta_1 - \beta - 1}, \quad x = D|t|^\nu \rightarrow \infty. \tag{18}
 \end{aligned}$$

Since $\beta_1 < 1 + \beta$, the exponent of $(-t)$ is negative, and thus for the considered limit the slope diverges (i.e., varying t at very large but fixed D). However, this limit does not include the limiting slope at $T \rightarrow T_c(D)$ itself, since then Eqs. (2) and (11) yield $t \propto D^{-1/\nu}$, and hence,

$$\tan(\theta) \propto H_1 D^{-(\beta_1 - \beta - 1)/\nu - 1} = H_1 D^{-(\Delta - \Delta_1 - 1)/\nu}. \tag{19}$$

In Landau theory, $\Delta = 3/2$, $\Delta_1 = 1/2$ and, hence, the power of D vanishes, i.e., the slope is nonzero and finite at $T_c(D)$ in the limit $D \rightarrow \infty$. For the three-dimensional Ising model, the best available exponent estimates^{50,19,51-53} imply $(\Delta - \Delta_1 - 1)/\nu \approx 0.12-0.16$, i.e., $\theta \rightarrow 0$ for $D \rightarrow \infty$! This result also implies that for capillary condensation field mixing effects⁸⁵ are asymptotically not very important.

We now briefly consider the extension of the scaling theory to include finite-size effects due to the finite lateral linear dimension L [in Eqs. (13) and (14) we have assumed the limit $L \rightarrow \infty$ throughout]. This can simply be done by including the aspect ratio L/D as an additional scaling variable in Eqs. (8) and (9), which we then rewrite as follows:

$$f_{\text{sing}}(D, T, H, H_1, L) \approx D^{-3} \tilde{f}(D^{1/\nu} t, L/D, HD^{\Delta/\nu}, H_1 D^{\Delta_1/\nu}). \tag{20}$$

Since for finite L the free energy and its derivatives are smooth functions of t , it is more convenient to use $D^{1/\nu} t$ rather than $x = D|t|^\nu$ as a scaling variable. From Eq. (20), we immediately obtain the following scaling results for the specific heat, the magnetization and the susceptibility of the thin film

$$C_v = D^{\alpha/\nu} \tilde{C}(D^{1/\nu} t, L/D, HD^{\Delta/\nu}, H_1 D^{\Delta_1/\nu}), \tag{21}$$

$$m = D^{-\beta/\nu} \tilde{m}(D^{1/\nu} t, L/D, HD^{\Delta/\nu}, H_1 D^{\Delta_1/\nu}), \tag{22}$$

$$\chi = D^{\gamma/\nu} \tilde{\chi}(D^{1/\nu} t, L/D, HD^{\Delta/\nu}, H_1 D^{\Delta_1/\nu}), \tag{23}$$

where \tilde{C} , \tilde{m} and $\tilde{\chi}$ are appropriate scaling functions. Since we choose H_1 fixed, D fixed, $H_1 D^{\Delta_1/\nu} \ll 1$, and H is chosen according to Eqs. (16) and (17) (in practice this is done by applying the reweighting technique and the equal area rule, cf. Fig. 3) the last two arguments $HD^{\Delta/\nu}$, $H_1 D^{\Delta_1/\nu}$ in Eqs. (21)–(23) can be ignored in the following discussion.

Now in the limit $L \rightarrow \infty$ we expect that C_v exhibits a logarithmic singularity for $T \rightarrow T_c(D)$, while the critical part of the magnetization $m_{\text{crit}} \equiv m - m(T_c(D), H, H_1)$ should behave as⁶²

$$m_{\text{crit}} \propto [1 - T/T_c(D)]^{\beta_2}, \quad \beta_2 = 1/8, \tag{24}$$

and the susceptibility

$$\chi \propto |1 - T/T_c(D)|^{-\gamma_2}, \quad \gamma_2 = 7/4. \tag{25}$$

For finite L , however, these singularities are all rounded off and we rather expect that both C_v and χ exhibit maxima of finite height at temperatures $T_{\text{max}}^c(D)$, $T_{\text{max}}^x(D)$. From Eqs. (21) and (23), we readily predict (in the limit $|H_1| D^{\Delta_1/\nu} \ll 1$):

$$\frac{T_{\text{max}}^c(D) - T_c(D)}{T_c(\infty)} D^{1/\nu} = \Delta \tilde{T}_{\text{max}}^c(L/D), \tag{26}$$

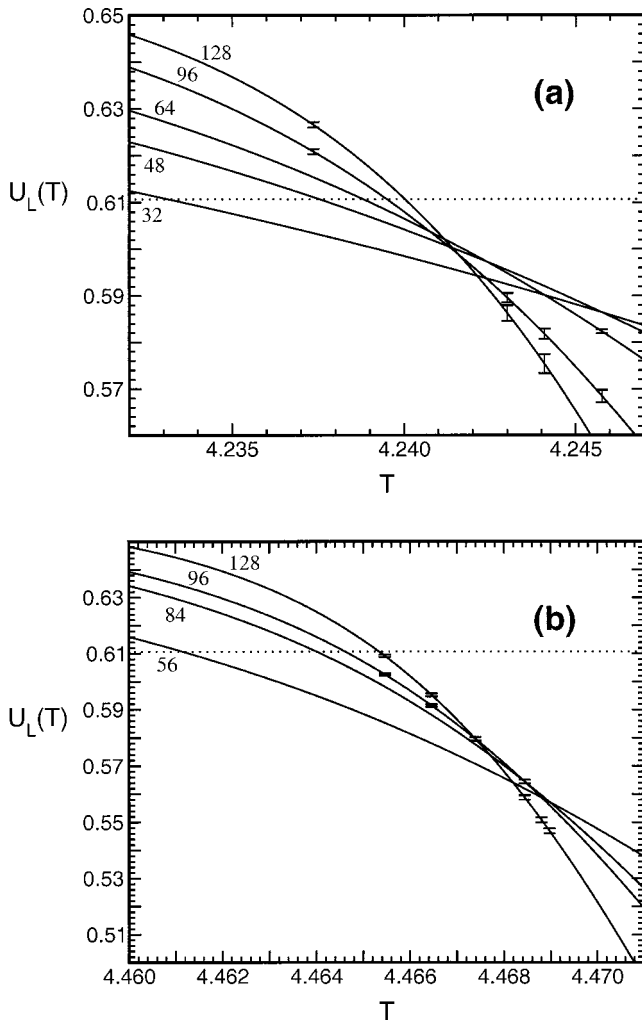


FIG. 4. Cumulants $U_L(T)$ plotted vs T for $D=8$ (a) and $D=28$ (b), for various choices of L as indicated in the figures. Dotted horizontal straight lines indicate the theoretical value U^* taken from Ref. 87.

$$\frac{T_{\max}^X(D) - T_c(D)}{T_c(\infty)} D^{1/\nu} = \Delta \tilde{T}_{\max}^X(L/D), \quad (27)$$

with $\Delta \tilde{T}_{\max}^c(L/D)$, $\Delta \tilde{T}_{\max}^X(L/D)$ being suitable scaling functions that describe the shift of these maxima positions as functions of the aspect ratio L/D . From this analysis one also can predict⁵⁸ how the height of the maxima should depend on D and L , for $L \gg D$:

$$C_v^{\max} \propto D^{\alpha/\nu} \ln(L/D), \quad (28)$$

$$\chi^{\max} \propto D^{\gamma/\nu - 7/4} L^{7/4}, \quad (29)$$

and how the absolute value of the order parameter should decrease at $T_c(D)$,

$$\langle |m_{\text{crit}}| \rangle_{T=T_c(D)} \propto D^{1/8 - \beta/\gamma} L^{-1/8}. \quad (30)$$

Finally, in the limit $L \rightarrow \infty$ the D dependence of the critical amplitudes associated with the two-dimensional critical behavior (see Ref. 58 for a more detailed discussion), defining now $\tilde{t} = [T - T_c(D)]/T_c(\infty)$, can be read off from the following equations:

$$C_v \propto D^{\alpha/\nu} \ln|\tilde{t}|, \quad (31)$$

$$m_{\text{crit}} \propto D^{(1/8 - \beta)/\nu} (-\tilde{t})^{1/8}, \quad (32)$$

$$\chi \propto D^{(\gamma - 7/4)/\nu} |\tilde{t}|^{-7/4}. \quad (33)$$

Due to the crossover scaling between two- and three-dimensional critical behavior, that Eqs. (20), (21), (22), and (23) describe, a singular dependence of the various critical amplitudes on film thickness results at the capillary condensation critical point.

IV. NUMERICAL RESULTS ON $T_c(D)$ AND $H_c(D)$

For locating critical points in the bulk, a convenient method is to study the fourth order cumulant of the order parameter

$$U_L(T) = 1 - \langle m_{\text{crit}}^4 \rangle / [3 \langle m_{\text{crit}}^2 \rangle^2] \quad (34)$$

for a range of linear dimensions L as a function of temperature, and to look for a common intersection point⁸⁶ [which for the universality class of the two-dimensional Ising model, should have the value⁸⁷ $U^* = U_L(T=T_c) = 0.610690(1)$]. In our case, we have to follow a path along $H = H_{\text{coex}}(T)$ [as shown in Fig. 3(b)] when we record these cumulants, and since this path is not exactly known but only within some numerical error, it is clear that this method is more difficult to apply than for ordinary bulk Ising models. In addition, even for small D the data are plagued by crossover scaling effects (Fig. 4): the curves for the values of L that are practically available do not intersect in a common point, but rather the intersection points are scattered and fall below the theoretical value U^* . This failure of verifying the common intersection points is not unexpected, since Fig. 4 includes data for which the aspect ratio L/D is as small as four (a) or even two (b), rather than only data for which $L/D \gg 1$. In fact, from the treatment of the previous section we can readily conclude that

$$U_L(T=T_c(D)) = \tilde{U}(L/D) \quad (35)$$

and only in the limit $L/D \rightarrow \infty$ shall we have $U(\infty) = U^*$.

An alternative and widely used recipe to find the critical temperature is to try an extrapolation of the maxima of the specific heat and susceptibility versus $L^{-1/\nu}$ or of the cumulant intersection points. Considering the intersection of $U_L(T)$ and $U_{bL}(T)$ with a scale factor $b > 1$, it can be argued⁸⁶ that corrections to finite-size scaling lead to a shift of the intersection point that varies with b proportional to $[b^{1/\nu} - 1]^{-1}$ for large b . Figure 5 shows some attempts to carry out such extrapolations, again for $D=8$ and $D=28$ (data for all other choices of D can be found in Ref. 76 and look similar). These figures show that T_{\max}^c approaches $T_c(D)$ in a nonmonotonic fashion, and also the curve T_{\max}^X vs $L^{-1/\nu}$ is distinctly nonlinear. Fitting asymptotic straight lines to both data sets one obtains results for $T_c(D)$ that are roughly compatible with each other, and with the (linear) extrapolation of the cumulant intersections. Although the accuracy of $T_c(D)$ obtained in this way is several orders of magnitude less than in the case of the bulk three-dimensional Ising model,⁸⁸ the data are accurate enough to allow a useful test of Eqs. (1) and (2).

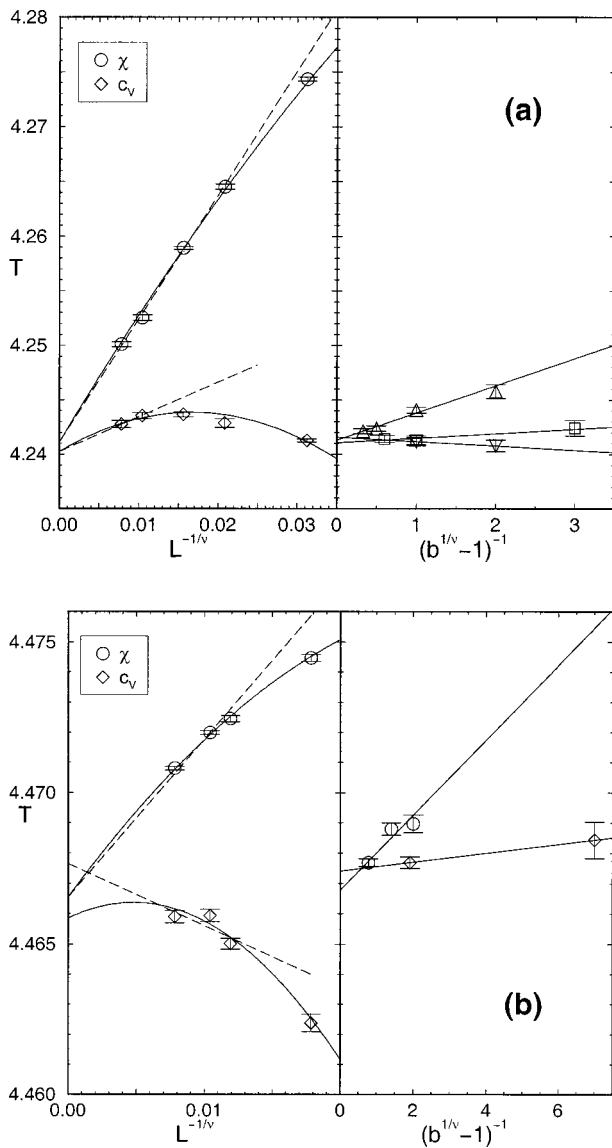


FIG. 5. Temperatures of specific heat and susceptibility maxima (left part) plotted vs $L^{-1/\nu}$, and temperatures of cumulant intersections plotted vs $(b^{1/\nu}-1)^{-1}$ (right part), for $D=8$ (a) and $D=28$ (b). In the left part the dashed curves show straight line fits and the solid curves correspond to the master curves in Fig. 6.

The consistency of our analysis can be checked further by testing for the scaling behavior predicted in Eqs. (26) and (27), see Fig. 6. Here all data points are included for all values of D and L that have been studied and $T_c(D)$ is chosen such that the best data collapse is achieved. It is seen that the nonmonotonic variation of the temperature at which the specific heat has its maximum is an intrinsic property of this scaling function describing the system shape effects in terms of the aspect ratio D/L of the simulation box. The interpolating curves are simple parabolic fits which translate back into the solid lines in the left part of Fig. 5.

The values of $T_c(D)$ that we have determined as shown in Figs. 5 and 6 are collected in Table I, which includes also our estimates for $H_c(D)$. Log-log plots of these data versus D almost look like straight lines, however, there is a slight but systematic curvature, and if this curvature were disregarded and straight lines were fitted to all the data neverthe-

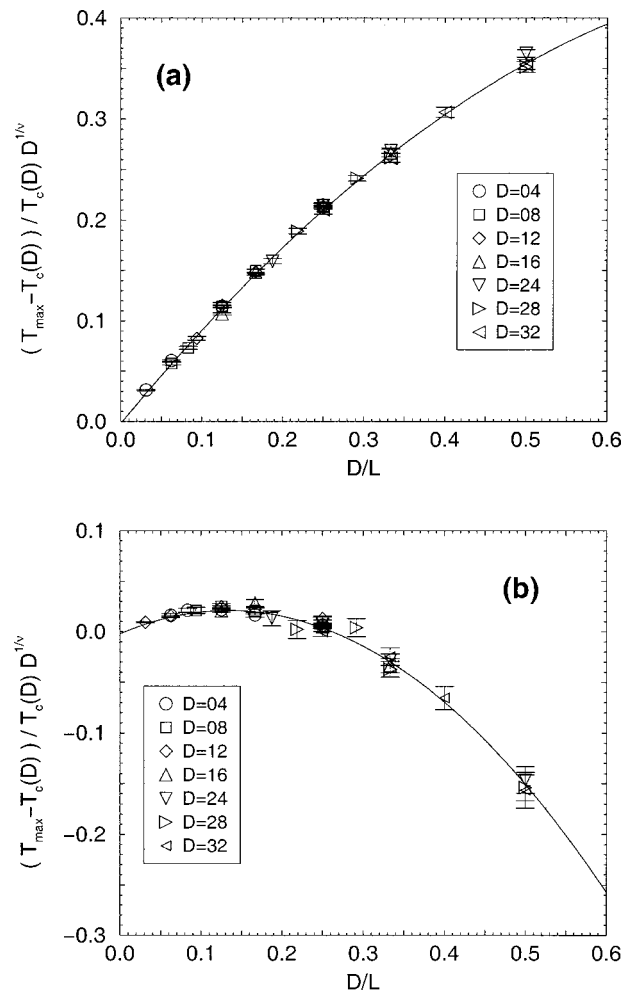


FIG. 6. Master curves for temperature of the susceptibility maxima (upper part) and specific heat maxima (lower part) plotted vs the inverse aspect ratio.

less, the resulting effective exponents would systematically deviate from the theoretical predictions in Eqs. (1) and (2).

Better results are obtained if one fits effective exponents from successive thicknesses only ($D=4,8,12$; $D=8,12,16$; ...; $D=24,28,32$), which can be extrapolated versus $1/D$ reasonably well, and converge nicely towards the theoretical predictions (Fig. 7), namely $-1/\nu \approx -1.587$ and $-(\Delta - \Delta_1)/\nu \approx -1.75$. Conversely, if Fig. 7(b) was taken as an independent estimation of the exponent Δ_1 , we would obtain $\Delta_1 = 0.459(13)$, which indeed is compatible with the existing recent estimates.⁵¹⁻⁵³

TABLE I. Critical temperatures and fields.

D	$T_c(D)$	$H_c(D)/J$
4	3.8705(3)	0.006 644(32)
8	4.2409(3)	0.002 528(14)
12	4.3561(3)	0.001 367(10)
16	4.4084(3)	0.000 867(6)
24	4.4549(5)	0.000 448(3)
28	4.4665(4)	0.000 348(3)
32	4.4749(5)	0.000 279(3)
∞	4.511 52(2)	0

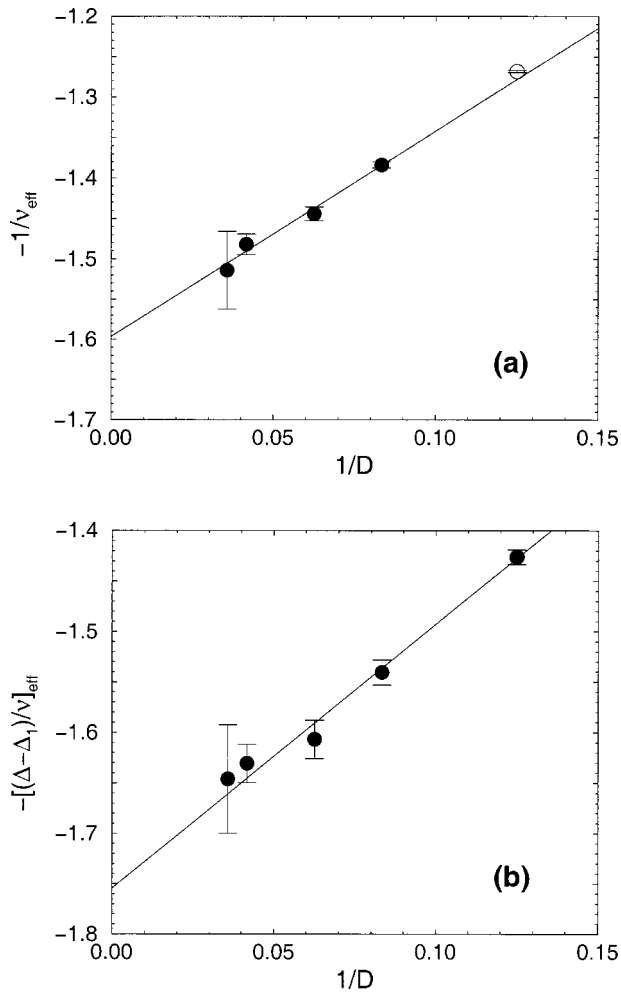


FIG. 7. Plot of $-1/\nu_{\text{eff}}$ (a) and $-[(\Delta-\Delta_1)/\nu]_{\text{eff}}$ (b) vs $1/D$ (effective exponents were fitted from three successive values of D).

V. A TEST OF TWO-DIMENSIONAL CRITICAL BEHAVIOR

In this section, we are concerned with the question to what extent the data provide some evidence for the prediction [Eq. (3)] that the capillary condensation critical point displays critical exponents of the two-dimensional Ising universality class. Since the accessible values of the lateral linear dimension L are not very large, however, we cannot expect that a regime can be reached where the parallel correlation length ξ_{\parallel} satisfies the criterion $D \ll \xi_{\parallel} \ll L$ —only in such a regime a direct observation of these power laws would be possible. Hence we attempt to study the critical behavior again via a finite-size scaling analysis, using^{10–14,18,54,55,66,67}

$$\langle |m_{\text{crit}}| \rangle L^{\nu} = \bar{M}(L^u \tilde{t}), \tag{36}$$

$$\chi L^{-w} = \tilde{\chi}(L^u \tilde{t}), \tag{37}$$

where the exponents u, v, w should take the values

$$u = 1/\nu_2 = 1, \quad v = \beta/\nu_2 = 1/8, \quad w = \gamma_2/\nu_2 = 7/4. \tag{38}$$

Equations (36), (37), and (38) are appropriate if $D \ll \xi_{\parallel}$ still holds but ξ_{\parallel} and L are of the same order. In practice, how-

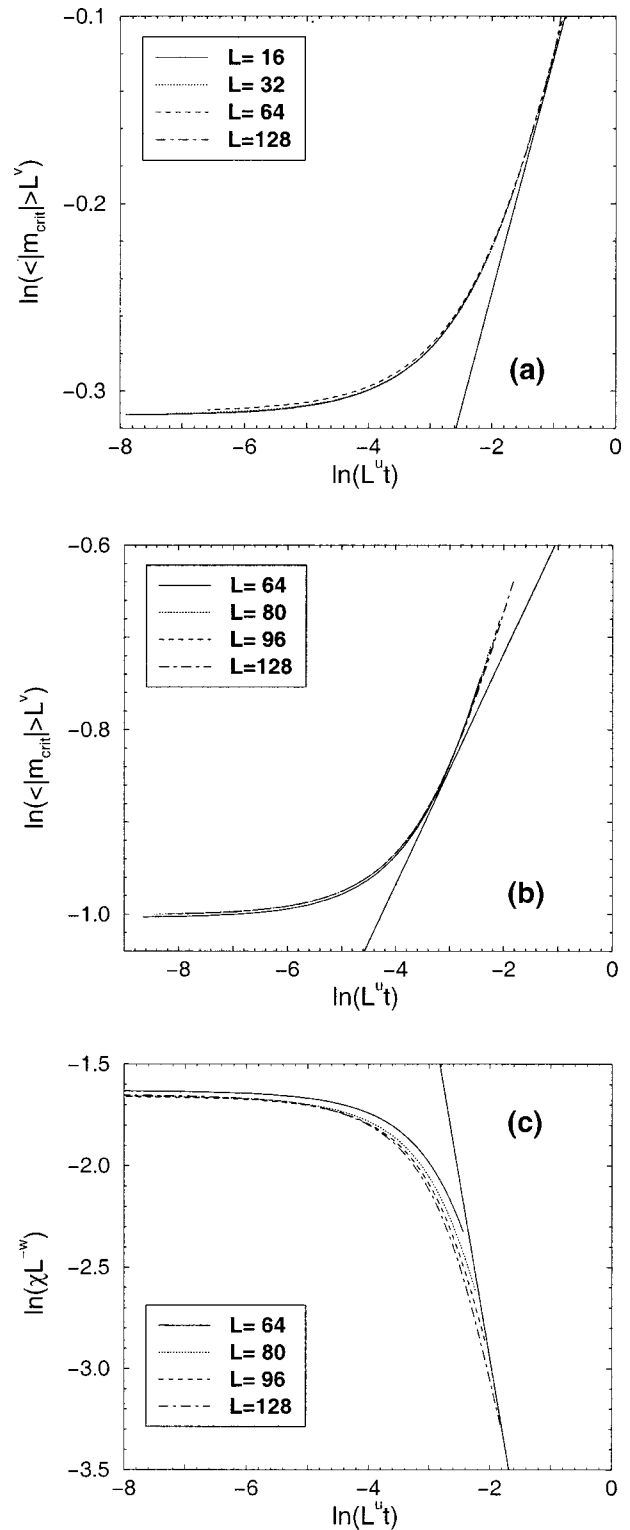


FIG. 8. (a) Finite-size scaling plot for the critical part of the magnetization, $\langle |m_{\text{crit}}| \rangle$, for $D=4$ and four choices of L as indicated, using $T_c(D)$ as quoted in Table I, and effective exponents $u=0.956, v=0.126$. The straight line has a slope indicating the exponent $\beta_2=1/8$. (b) Same as (a) but for $D=32$, using now $u=0.884, v=0.155$. (c) Same as (b) but for the susceptibility, using $u=0.884, w=1.55$. The straight line indicates the exponent $\gamma_2=7/4$.

ever, also the condition $D \ll \xi_{\parallel}$ is hard to satisfy since we wish to include some data for which L/D is not very large. It then helps to relax the theoretical condition, Eq. (38), and rather treat u, v, w as effective exponents:⁵⁸ in this way, one

TABLE II. Effective exponents for order parameter and susceptibility.

D 2-dim	u 1	v 1/8	w 7/4	β_{eff} 1/8	γ_{eff} 7/4	ν_{eff} 1
4	0.956	0.126	1.67	0.132	1.75	1.064
8	1.018	0.136	1.72	0.133	1.69	0.982
12	0.944	0.138	1.67	0.146	1.77	1.059
16	0.938	0.139	1.61	0.148	1.72	1.066
24	0.898	0.145	1.53	0.161	1.70	1.114
28	0.853	0.141	1.48	0.165	1.74	1.172
32	0.884	0.155	1.54	0.175	1.74	1.131
3-dim	1.587	0.518	1.96	0.327	1.24	0.630

can take into account to some extent the corrections to finite-size scaling arising from the crossover between two- and three-dimensional Ising critical behavior.

Figure 8 shows that this procedure works reasonably well, and Table II gives a listing of the fit exponents u , v , w , and corresponding effective exponents $\nu_{\text{eff}}=1/u$, $\beta_{\text{eff}}=v/u$, and $\gamma_{\text{eff}}=w/u$. It is seen from Table II that both u , v and w gradually change from the two-dimensional values towards the three-dimensional ones, although even for $D=32$ one is still far away from the theoretical values for the latter. While β_{eff} has increased significantly, γ_{eff} within the accuracy of this estimation has hardly changed at all. If we consider an effective dimensionality from the hyperscaling relation,⁶² defined as $d_{\text{eff}}=(\gamma_{\text{eff}}+2\beta_{\text{eff}})/\nu_{\text{eff}}=w+2v$, we find $d_{\text{eff}}=2.0 \pm 0.15$, and there is no systematic trend with D . While the latter observation is in accord with a previous study using ‘‘neutral walls,’’⁵⁸ where $H_c(D) \equiv 0$, we have obtained in the present work a much better evidence that for small D the behavior is compatible with two-dimensional Ising criticality than was possible in the latter model.⁵⁸ Note also that in the present study there is a rather broad range of D where $\nu_{\text{eff}} > 1$, which was not the case in Ref. 58. Due to the systematic problems of fitting several effective exponents from somewhat noisy data and the restricted range over which this fit is applicable we do not think that these discrepancies are a proof of nonuniversal crossover behavior, however. We feel that this problem needs a more careful study.

VI. CONCLUSIONS

In this paper Monte Carlo simulations have been presented attempting to test theoretical predictions about the capillary condensation critical point. Using an extension of the Swendsen–Wang cluster algorithm including competing surface and bulk magnetic fields, for Ising films with thicknesses $D=4, 8, 12, 16, 24, 28$, and 32 the critical temperature $T_c(D)$ and corresponding critical field $H_c(D)$ for a surface magnetic field H_1 have been estimated. The data are compatible with the power laws presented about 20 years ago by Fisher and Nakanishi. Also the expected two-dimensional critical behavior is compatible with our data, though the accuracy of the resulting effective exponents is rather low (Table II) and, hence, a more convincing proof would be desirable, but is not feasible with the present computer resources.

A challenging problem that we have not solved is the development of an efficient version of the cluster algorithm that allows to work with surface and bulk fields that are not extremely small. The algorithm that we have used was much less efficient even for $H_1 = -0.015J$ than for $H_1 = 0$, and a study of capillary condensation critical points over the range where $(H_1/J)D^{\Delta_1/\nu}$ is not small, and hence, the nonlinear part of the scaling function $Y_c(CH_1D^{\Delta_1/\nu})$ would be probed, turned out not to be feasible either. Thus, in spite of a long-standing effort to deal with theory and simulation of capillary condensation there remain still some missing links. A particularly intriguing problem is to elucidate the crossover between three-dimensional and two-dimensional critical behavior in these thin films. Finally, it is hoped that the present study provides an incentive to address this problem also by suitable experiments.

ACKNOWLEDGMENTS

One of us (O.D.) acknowledges support from the Deutsche Forschungsgemeinschaft (DFG) under Grant No. Bi314/16, another (W.J.) acknowledges support from the Heisenberg program of the DFG and from Sonderforschungsbereich 262/D1.

- ¹ *Liquids at Interfaces*, edited by J. Charvolin, J. F. Joanny, and J. Zinn-Justin, (Elsevier, Amsterdam, 1990).
- ² G. Krausch, *Mater. Sci. Eng., R.* **14**, 1 (1995).
- ³ K. Binder, *J. Non-Equilib. Thermodyn.* **23**, 1 (1998).
- ⁴ *Polymers in Confined Environments*, Adv. Polymer Sci. 138, edited by S. Granick (Springer, Berlin, 1999).
- ⁵ International Workshop on Dynamics in Confinement, edited by B. Frick, R. Zorn, and H. Büttner, *J. Phys. IV* **10** (2000).
- ⁶ *Fluid Interfacial Phenomena*, edited by C. A. Croxton (Wiley, New York 1986).
- ⁷ D. Henderson, *Fundamentals of Inhomogeneous Fluids* (Marcel Dekker, New York, 1992).
- ⁸ K. Binder, *Annu. Rev. Phys. Chem.* **43**, 33 (1992).
- ⁹ T. L. Hill, *Statistical Mechanics of Small Systems* (Benjamin, New York, 1956), Vols. 1 and 2.
- ¹⁰ M. E. Fisher, in *Critical Phenomena, Proceedings of the 1970 Enrico Fermi School of Physics, Course 51, Varenna, Italy*, edited by M. S. Green (Academic, New York, 1971), p. 1.
- ¹¹ K. Binder, *Physica (Utrecht)* **62**, 508 (1972).
- ¹² M. E. Fisher and M. N. Barber, *Phys. Rev. Lett.* **28**, 1516 (1972).
- ¹³ K. Binder, *Thin Solid Films* **20**, 367 (1974).
- ¹⁴ D. P. Landau, *Phys. Rev. B* **13**, 2997 (1976); **14**, 255 (1976).
- ¹⁵ M. E. Fisher and H. Au-Yang, *Physica A* **101**, 255 (1980); H. Au-Yang and M. E. Fisher, *Phys. Rev. B* **21**, 3956 (1980).
- ¹⁶ M. E. Fisher and H. Nakanishi, *J. Chem. Phys.* **75**, 5875 (1981).
- ¹⁷ H. Nakanishi and M. E. Fisher, *J. Chem. Phys.* **78**, 3279 (1983).
- ¹⁸ M. N. Barber, in *Phase Transitions and Critical Phenomena*, edited by C. Domb and J. L. Lebowitz (Academic, New York, 1983), Vol. 8, p. 145.
- ¹⁹ K. Binder, in *Phase Transitions and Critical Phenomena*, edited by C. Domb and J. L. Lebowitz (Academic, New York, 1983), Vol. 8, p. 1.
- ²⁰ R. Evans and P. Tarazona, *Phys. Rev. Lett.* **52**, 557 (1984).
- ²¹ R. Evans and U. M. B. Marconi, *Chem. Phys. Lett.* **114**, 415 (1985); *Phys. Rev. A* **32**, 3817 (1985).
- ²² R. Evans, U. M. B. Marconi, and P. Tarazona, *J. Chem. Phys.* **84**, 2376 (1986); *J. Chem. Soc., Faraday Trans. 2* **82**, 1763 (1986).
- ²³ P. Tarazona, U. M. B. Marconi, and R. Evans, *Mol. Phys.* **60**, 573 (1987); E. Bruno, U. M. B. Marconi, and R. Evans, *Physica A* **141**, 178 (1987).
- ²⁴ D. Nicolaidis and R. Evans, *Phys. Rev. B* **39**, 9336 (1989).
- ²⁵ J. P. R. B. Walton and N. Quirke, *Mol. Simul.* **2**, 361 (1989).
- ²⁶ E. V. Albano, K. Binder, D. W. Heermann, and W. Paul, *J. Chem. Phys.* **91**, 3700 (1989).
- ²⁷ R. Evans, *J. Phys.: Condens. Matter* **2**, 8989 (1990).
- ²⁸ K. Binder and D. P. Landau, *J. Chem. Phys.* **96**, 1444 (1992).

- ²⁹E. V. Albano, K. Binder, and W. Paul, *J. Phys. A* **30**, 3285 (1997).
- ³⁰M. Müller and K. Binder, *Macromolecules* **31**, 8323 (1998).
- ³¹C. Varea and A. Robledo, *Physica A* **268**, 391 (1999).
- ³²M. Müller, K. Binder, and E. V. Albano, *Europhys. Lett.* **50**, 724 (2000).
- ³³L. D. Gelb, K. E. Gubbins, R. Radhakrishnan, and M. Sliwinski-Bartkowiak, *Rep. Prog. Phys.* **62**, 1573 (1999).
- ³⁴W. T. Thomson (Lord Kelvin), *Philos. Mag.* **42**, 448 (1871).
- ³⁵S. J. Gregg and K. S. W. Sing, *Adsorption, Surface Area and Porosity* (Academic, New York, 1982).
- ³⁶D. T. Jacobs, R. C. Mockler, and W. J. O'Sullivan, *Phys. Rev. Lett.* **37**, 1471 (1976).
- ³⁷B. A. Scheibner, M. R. Meadows, R. C. Mockler, and W. J. O'Sullivan, *Phys. Rev. Lett.* **43**, 590, 592 (1979).
- ³⁸C. G. V. Burgess, D. H. Everett, and S. Nuttal, *Pure Appl. Chem.* **61**, 1845 (1989).
- ³⁹P. J. Branton, P. G. Hall, and K. S. W. Sing, *J. Chem. Soc. Chem. Commun.* **1993**, 1257.
- ⁴⁰W. D. Machin, *Langmuir* **10**, 1235 (1994); **15**, 169 (1999).
- ⁴¹P. I. Rakikovitch, S. C. O. Domhnaill, A. V. Neimark, F. Schüth, and K. K. Unger, *Langmuir* **11**, 4765 (1995).
- ⁴²J. Rathousky, A. Zukal, O. Franke, and G. Schulz-Ekloff, *J. Chem. Soc., Faraday Trans.* **91**, 937 (1995).
- ⁴³M. Thommes, G. H. Findenegg, and M. Schön, *Langmuir* **11**, 2137 (1995).
- ⁴⁴J. H. Page, J. Liu, B. Abeles, H. W. Deckman, and D. A. Weitz, *Phys. Rev. Lett.* **71**, 1216 (1996).
- ⁴⁵S. Gross and G. H. Findenegg, *Ber. Bunsenges. Phys. Chem.* **101**, 1726 (1997).
- ⁴⁶P. J. Branton, K. S. W. Sing, and J. W. White, *J. Chem. Soc., Faraday Trans.* **93**, 2337 (1997).
- ⁴⁷M. Kruk, M. Jaroniec, and A. Sayari, *Langmuir* **13**, 6267 (1997).
- ⁴⁸Y. Long, T. Xu, Y. Sun, and W. Dong, *Langmuir* **14**, 6173 (1998).
- ⁴⁹K. Morishige and M. Shikimi, *J. Chem. Phys.* **108**, 7821 (1998).
- ⁵⁰J. C. LeGuillou and J. Zinn-Justin, *Phys. Rev. B* **21**, 3976 (1980).
- ⁵¹K. Binder and D. P. Landau, *Phys. Rev. Lett.* **52**, 318 (1984); *Physica A* **163**, 17 (1990); D. P. Landau and K. Binder, *Phys. Rev. B* **41**, 4633 (1990).
- ⁵²C. Ruge, S. Dunkelmann, F. Wagner, and J. Wulf, *J. Stat. Phys.* **73**, 293 (1993); C. Ruge and F. Wagner, *Phys. Rev. B* **52**, 4209 (1995).
- ⁵³H. W. Diehl and M. Shpot, *Nucl. Phys. B* **528**, 595 (1998).
- ⁵⁴*Finite Size Scaling and the Numerical Simulation of Statistical Systems*, edited by V. Privman (World Scientific, Singapore, 1990).
- ⁵⁵K. Binder, in *Computational Methods in Field Theory*, edited by H. Gaus-terer and C. B. Lang (Springer, Berlin, 1992), p. 59.
- ⁵⁶T. W. Capehart and M. E. Fisher, *Phys. Rev. B* **13**, 6021 (1976).
- ⁵⁷F. Freire, D. O'Connor, and C. R. Stephens, *J. Stat. Phys.* **74**, 219 (1994); D. O'Connor and C. R. Stephens, *Phys. Rev. Lett.* **72**, 506 (1994).
- ⁵⁸Y. Rouault, J. Baschnagel, and K. Binder, *J. Stat. Phys.* **80**, 1009 (1995).
- ⁵⁹P. Schilbe, S. Siebentritt, and K.-H. Rieder, *Phys. Lett. A* **216**, 20 (1995).
- ⁶⁰M. I. Marqués and J. A. Gonzalo, *Eur. Phys. J. B* **14**, 317 (2000).
- ⁶¹A. O. Parry and R. Evans, *J. Phys. A* **25**, 275 (1992).
- ⁶²M. E. Fisher, *Rev. Mod. Phys.* **46**, 587 (1974).
- ⁶³S. Dietrich, in *Phase Transitions and Critical Phenomena*, edited by C. Domb and J. L. Lebowitz (Academic, New York, 1988), Vol. 12, p. 1.
- ⁶⁴K. Binder and D. P. Landau, *J. Appl. Phys.* **57**, 3306 (1985); *Phys. Rev. B* **37**, 1745 (1988); K. Binder, D. P. Landau, and S. Wansleben, *ibid.* **40**, 6971 (1989).
- ⁶⁵N. Metropolis, A. W. Rosenbluth, M. N. Rosenbluth, A. H. Teller, and E. Teller, *J. Chem. Phys.* **21**, 1087 (1953).
- ⁶⁶K. Binder, *Rep. Prog. Phys.* **60**, 487 (1997).
- ⁶⁷D. P. Landau and K. Binder, *A Guide to Monte Carlo Simulations in Statistical Physics* (Cambridge University Press, Cambridge, 2000).
- ⁶⁸A. Milchev, K. Binder, and D. W. Heermann, *Z. Phys. B: Condens. Matter* **63**, 521 (1986).
- ⁶⁹R. H. Swendsen and J. S. Wang, *Phys. Rev. Lett.* **58**, 86 (1987).
- ⁷⁰U. Wolff, *Phys. Rev. Lett.* **62**, 361 (1989).
- ⁷¹J. S. Wang, *Physica A* **161**, 249 (1989).
- ⁷²P. G. Lauwers and V. Rittenberg, *Phys. Lett. B* **233**, 197 (1989).
- ⁷³V. S. Dotsenko, W. Selke, and A. L. Talapov, *Physica A* **170**, 278 (1990).
- ⁷⁴R. H. Swendsen, J. S. Wang, and A. M. Ferrenberg, in *The Monte Carlo Method in Condensed Matter Physics*, edited by K. Binder (Springer, Berlin, 1992), p. 75.
- ⁷⁵W. Janke, in *Computational Physics: Selected Methods, Simple Exercises, Serious Applications*, edited by K. H. Hoffmann and M. Schreiber (Springer, Berlin, 1996), p. 10.
- ⁷⁶O. Dillmann, Dissertation, Johannes-Gutenberg-Universität, Mainz, 2000 (unpublished).
- ⁷⁷A very brief account on this point demonstrating test results was given by us in O. Dillmann, M. Müller, W. Janke, and K. Binder, in *Computer Simulation Studies in Condensed Matter Physics XII, Springer Proceedings in Physics* Vol. 85, edited by D. P. Landau, S. P. Lewis and H. B. Schüttler (Springer, Berlin, 2000), p. 124.
- ⁷⁸H. Flyvbjerg and H. G. Peterson, *J. Chem. Phys.* **91**, 461 (1989).
- ⁷⁹A. Ferrenberg, D. P. Landau, and Y. J. Wong, *Phys. Rev. Lett.* **69**, 3382 (1992).
- ⁸⁰S. Kirkpatrick and E. P. Stoll, *J. Comp. Physiol.* **40**, 517 (1981).
- ⁸¹A. M. Ferrenberg and R. H. Swendsen, *Phys. Rev. Lett.* **63**, 1195 (1989).
- ⁸²K. Binder and D. P. Landau, *Phys. Rev. B* **30**, 1477 (1984); C. Borgs and R. Kotecky, *J. Stat. Phys.* **61**, 79 (1990); C. Borgs, R. Kotecky, and S. Miracle-Sole, *ibid.* **62**, 529 (1991); C. Borgs and W. Janke, *Phys. Rev. Lett.* **68**, 1738 (1992); W. Janke, *Phys. Rev. B* **47**, 14753 (1993).
- ⁸³B. Efron, *The Jackknife, the Bootstrap and Other Resampling Plans* (SIAM, Philadelphia, 1982).
- ⁸⁴K. Binder and P. C. Hohenberg, *Phys. Rev. B* **6**, 3461 (1972); **9**, 2194 (1974).
- ⁸⁵A. D. Bruce and N. B. Wilding, *Phys. Rev. Lett.* **68**, 193 (1992).
- ⁸⁶K. Binder, *Phys. Rev. Lett.* **47**, 693 (1981); *Z. Phys. B: Condens. Matter* **43**, 119 (1981).
- ⁸⁷G. Kamieniarz and H. W. J. Blöte, *J. Phys. A* **26**, 201 (1993).
- ⁸⁸H. W. J. Blöte, E. Luijten, and J. R. Heringa, *J. Phys. A* **28**, 6289 (1995); D. P. Landau, *Physica A* **205**, 41 (1994).